metals

MDPI

Article

CNN-Based Microstructural Carbide Detection in Stainless Steel: Effects of Dataset Size

Fuad Khoshnaw * and Weigang Yao

School of Engineering, Infrastructure and Sustainability, De Montfort University, Leicester LE1 9BH, UK; weigang.yao@dmu.ac.uk

* Correspondence: fuad.khoshnaw@dmu.ac.uk

Abstract

This study developed a machine learning approach to detect carbide precipitation in the microstructure of austenitic stainless steel, specifically grade 316, using a convolutional neural network (CNN). Microstructural images were prepared and classified into three categories: as-received, heat-treated without carbide precipitation, and heat-treated with carbide precipitation. A CNN was trained and validated using two separate datasets of varying sizes to assess the impact of data quantity on classification performance. This automated microstructure recognition system offers potential benefits for additive manufacturing (AM) by enabling real-time quality assessment and feedback control, particularly for avoiding undesirable carbide formation during metal 3D printing. By linking microstructural analysis to processing conditions, this approach supports the development of defect-free, corrosion-resistant components and contributes to the integration of intelligent monitoring within digital manufacturing workflows.

Keywords: machine learning; carbide detection; austenitic st. st.; microstructure analysis; additive manufacturing

1. Introduction

In this century, humanity faces critical challenges, including intense global competition, growing human demands, and population expansion, all of which stress limited resources. As a result, achieving sustainable manufacturing has become a global priority. One strategy gaining momentum is the concept of "FabLab", which focuses on rapid prototyping and evaluation of full-scale product feasibility.

Among the key technologies supporting this approach is additive manufacturing (AM), which draws on principles derived from welding processes to build components layer by layer. Prior work by the author [1,2] focused on adapting traditional welding systems, such as Gas Tungsten Arc Welding (GTAW) and Gas Metal Arc Welding (GMAW), to maintain constant torch speed and controlled heat input. In a separate study [3], the author investigated carbide formation and other phase transformations, such as sigma (σ) phase precipitation in stainless steel alloys. These aspects are critical for AM, as they directly influence the controlled deposition of molten feedstock and the fabrication of large metallic structures [4].

AM technologies that utilise arc welding as a heat source and metal wires as feedstock offer advantages such as high deposition rates, low setup costs, and material diversity [5,6]. However, complexities in arc behaviour, heat transfer, bead geometry (e.g., width, height,

Check for updates

Academic Editor: Andrea Di Schino

Received: 19 March 2026
Revised: 9 April 2026
Accepted: 12 April 2026
Published: 14 April 2026

Copyright: © 2026 by the authors. Licensee MDPI, Basel, Switzerland. This article is an open access article distributed under the terms and conditions of the Creative Commons Attribution (CC BY) license.

penetration), and heat input make it difficult to control the process consistently [7]. Consequently, despite significant advancements, AM remains largely at the laboratory scale, with limited adoption in industrial settings. Addressing this gap, artificial intelligence (AI) techniques are increasingly being explored to enhance process control and product quality.

One of the major challenges in metal AM lies in microstructural evolution during printing, which significantly impacts mechanical and corrosion properties. High thermal gradients and repeated heating cycles in AM can trigger undesirable transformations such as phase changes and carbide or second-phase precipitation. For instance, austenitic stainless steels like AISI 304 are prone to chromium carbide precipitation within the sensitisation range (550–850 °C), causing intergranular corrosion. Similarly, duplex stainless steels require a stable ferrite-to-austenite ratio to preserve strength and corrosion resistance, while aluminium alloys rely on post-weld ageing to regain hardness [2]. Managing such transformations manually is difficult without intelligent monitoring and control systems.

Liu et al. [8] summarised AM progress, including materials development, deposition strategy, and real-time monitoring using multisensory systems. These advancements highlight the importance of integrating AI technologies to manage complexity in AM. Data-driven approaches, including machine learning techniques such as regression models, have been applied in materials engineering to model relationships between material parameters and performance [9]. Lee et al. [10] used high-dynamic-range imaging to classify defects in AM via AI models, achieving up to 99% accuracy. Similarly, Li et al. [11] implemented an image-based detection system using YOLOv3 to identify anomalies such as lack of fusion and voids, offering high precision in real-time layer evaluation.

Tang et al. [12] developed a topography-based monitoring approach for closed-loop control, while Xia et al. [13] outlined sensor-based feedback mechanisms for improving AM reliability. Barrionuevo et al. [4] assessed various machine learning (ML) algorithms to predict bead geometry in plasma arc deposition of Ti-6Al-4V. However, Xiao et al. [7] noted limitations in traditional ML models when accounting for interdependent variables and proposed an advanced framework for more accurate prediction of deposition shapes. Oh et al. [14] employed support vector machines to identify optimal conditions for bead uniformity, achieving minimal geometry errors. Kunchala et al. [15] introduced a hybrid ML model combined with IoT technologies for process optimisation. Ding et al. [16] proposed a complete modelling system for parameter selection using SVMs to control wire feed rate and travel speed with high precision. Abdalel et al. [17] reviewed the application of AI, particularly machine learning and computer vision, in SEM and EDS-based microstructural analysis. Their work highlights automated and accurate detection of microstructural features, aligning with the present study's use of AI for carbide detection and its potential for advanced manufacturing applications.

While much progress has been made, current research has primarily focused on predicting deposition geometry or detecting macro-level defects. Less attention has been paid to recognising microstructural features, such as chromium carbide precipitation, which are critical for the corrosion performance of AM-fabricated stainless steels. Manual metallography is slow and inefficient for production environments.

Although many previous studies have applied AI and ML in additive manufacturing, the integration of image-based microstructure recognition for carbide detection remains underexplored. This study addresses this gap by developing a machine learning model to classify metallographic images of austenitic stainless steel based on carbide presence. This study focuses on image-based microstructure classification and does not incorporate process parameters; however, it provides a foundation for future integration with process–structure relationships in additive manufacturing.

2. Methodology

This study utilises a supervised deep learning approach to classify microstructure images of austenitic stainless steel into three categories: as-received, heat-treated without carbide precipitation, and heat-treated with carbide precipitation. The full workflow involves data preparation, CNN model development, training, evaluation, and comparative analysis between two image dataset sizes.

2.1. Dataset and Image Preparation

Microscopic images were collected under consistent magnification and illumination conditions. The dataset was manually organised into three class folders representing the three conditions. Images were resized to 128×128 pixels and normalised to a $[0, 1]$ range using rescaling to ensure computational efficiency while preserving essential microstructural features. Higher resolutions were considered; however, they did not provide a noticeable improvement in model performance relative to the increased computational cost. The dataset size is limited, and therefore, the present study is intended as a proof-of-concept for image-based microstructure classification.

Two experimental runs were performed:

In the initial experimental run (Run 1—Baseline), the model was trained on a relatively limited dataset comprising a total of 34 images. The training set included 4 images of as-received microstructures, 15 images of heat-treated samples without carbide precipitation, and 15 images of heat-treated samples with carbide precipitation. For evaluation, the test set contained 7 images in total: 1 as-received image, 3 heat-treated images without carbides, and 3 with carbide precipitation. This configuration was designed to establish a baseline for model performance with a minimal number of images per class.

In the second experimental run (Run 2—Expanded Dataset), the training and test datasets were enhanced to improve model generalisation and classification performance. The training set included a total of 40 images: 10 as-received microstructure images, 15 heat-treated images without carbide precipitation, and 15 heat-treated images with carbide precipitation. The test set was significantly expanded to include 30 images in total, with 10 images for each of the three classes. This increased dataset size was intended to provide a more balanced and representative sample distribution, allowing the model to learn more robust microstructural features associated with carbide presence and absence.

The dataset was divided into training and testing sets. During model training, the test set was also used as validation data to monitor model performance and reduce overfitting. Although deep learning models typically benefit from large datasets, this study demonstrates that a moderate number of high-quality images (40 training and 30 testing) is sufficient to train a CNN for recognising carbide precipitation in austenitic stainless-steel microstructures. The dataset was carefully curated and well-labelled into three visually distinct classes, thereby reducing noise and ambiguity and minimising the need for large-scale data. Furthermore, a lightweight CNN architecture with fewer parameters was employed to prevent overfitting, thereby enabling effective learning from limited sample sizes. This work serves as a proof-of-concept study, showing that even with a small dataset, meaningful classification accuracy can be achieved, with future improvements anticipated through data augmentation and larger datasets.

The directory structure was consistent across runs:

```
bash
CopyEdit
microstructure_dataset/
    train/
        as_received/
```

```
        heat_treated_no_carbides/
        heat_treated_with_carbides/
    test/
        as_received/
        heat_treated_no_carbides/
        heat_treated_with_carbides/
```

2.2. Model Architecture

A custom CNN model was implemented in TensorFlow/Keras [18], consisting of
Conv2D layer (16 filters, 3 × 3, ReLU);
MaxPooling2D layer;
Conv2D layer (32 filters, 3 × 3, ReLU);
MaxPooling2D layer;
Flatten layer;
Dense layer (64 units, ReLU);
Output dense layer (Softmax for 3-class classification).

2.3. Training Configuration

Loss Function: Categorical cross-entropy.
Optimizer: Adam.
Metrics: Accuracy.
Epochs:
Run 1: 10 epochs;
Run 2: 30 epochs.
ImageDataGenerator was used for rescaling and batching (no data augmentation).

2.4. Evaluation Metrics

Accuracy and loss curves were plotted and saved using matplotlib.
Model output was saved in .keras format.
A confusion matrix and classification report were generated using scikit-learn to assess precision, recall, and F1-score.
Output Directory: All results are saved to the results/folder for analysis and documentation.

2.5. Microstructure Categories

To support the development of the classification model, a set of metallographic images was prepared from austenitic stainless-steel grade 316 specimens subjected to different heat treatment conditions, to reach the heat-affected zone (HAZ), and holding the samples for different times to form chromium carbide precipitation. To proceed with microstructural investigations, samples were prepared following grinding, polishing, and etching. Then, immersion in a solution of 10 mL HCL, 5 mL HNO_3, and distilled water for 4 min was applied. Microstructural images were obtained from samples in the as-received (solution-annealed) condition and after heat treatment at different temperatures and holding times to produce distinct microstructural states. The use of controlled heat treatment conditions ensures clear differentiation between classes, which is essential for training a reliable classification model.

The samples were categorised into three distinct groups: (1) as-received, representing the baseline microstructure with uniform austenitic grains and clean grain boundaries; (2) heat-treated without carbide precipitation, where thermal exposure did not result in visible grain boundary carbides; and (3) heat-treated with carbide precipitation, showing clear carbide formations along grain boundaries, typically associated with sensitization

effects. Figure 1 shows these representative microstructures, which served as the visual basis for training and evaluating the machine learning model used in this study.

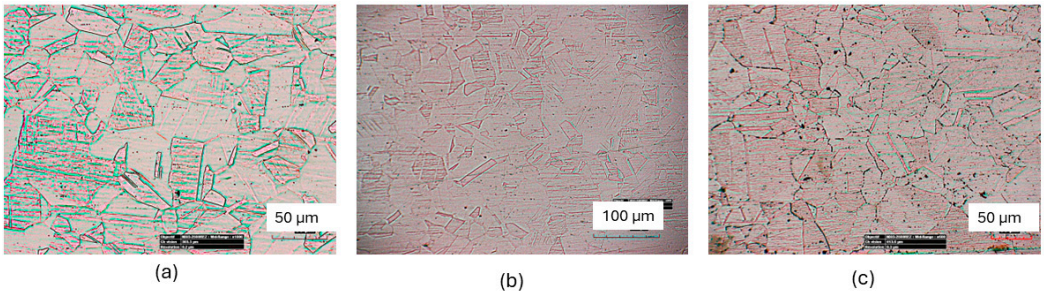


Figure 1. Representative microstructures of austenitic stainless steel: (**a**) as-received (solution-annealed condition), showing equiaxed austenitic grains with clean grain boundaries and no visible carbide precipitation; (**b**) solution annealed—with no visible carbide precipitation; (**c**) precipitation annealed—with visible carbide precipitates along grain boundaries. Source: author's own work.

2.6. Deep Learning Model Structure

To implement the image classification model, a convolutional neural network (CNN) was designed with a standard sequential architecture. Figure 2 shows the network begins with an input layer that accepts images resized to 128 × 128 pixels with three RGB channels. This is followed by convolutional and pooling layers to extract spatial features, a flattening layer to convert the 2D matrix into a 1D vector, and fully connected (dense) layers. The output layer uses a softmax activation function to classify the images into three categories: as-received, heat-treated without carbides, and heat-treated with carbide precipitation.

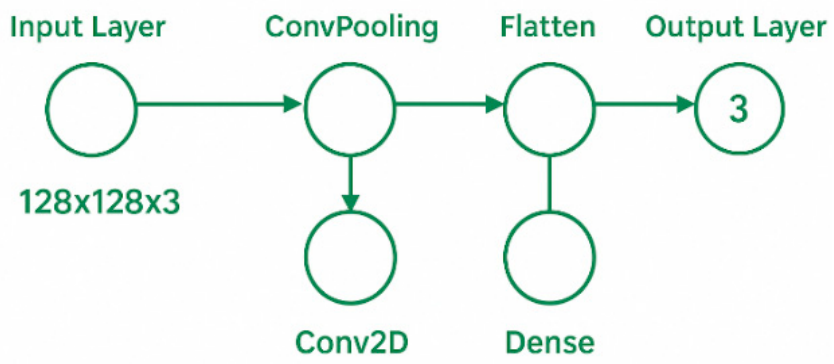


Figure 2. Architecture of the convolutional neural network (CNN) used for classifying microstructural images into three categories. The model includes Conv2D, pooling, flatten, and dense layers with an output layer of 3 classes. Source: author's own work.

3. Results and Discussion

The training and evaluation processes were conducted in two phases, corresponding to two different dataset sizes. Each run was evaluated by analysing the training and validation accuracy across epochs, in addition to using classification metrics such as precision, recall, and F1-score. The aim was to assess the model's ability to distinguish between three classes of microstructure images: as-received, heat-treated without carbide precipitation, and heat-treated with carbide precipitation. The inclusion of the as-received condition allows the model to distinguish baseline microstructures from thermally altered states, which is essential for accurate classification.

3.1. First Run—Baseline Model Performance

The first run used a limited dataset consisting of only 34 training images and seven testing images. The training was performed for 10 epochs. Figure 3 shows the model exhibited low performance, with validation accuracy stagnating around 42–57%, and high validation loss throughout. These results indicate that the model was underfitting, likely due to the insufficient number of training examples and limited variation in the dataset.

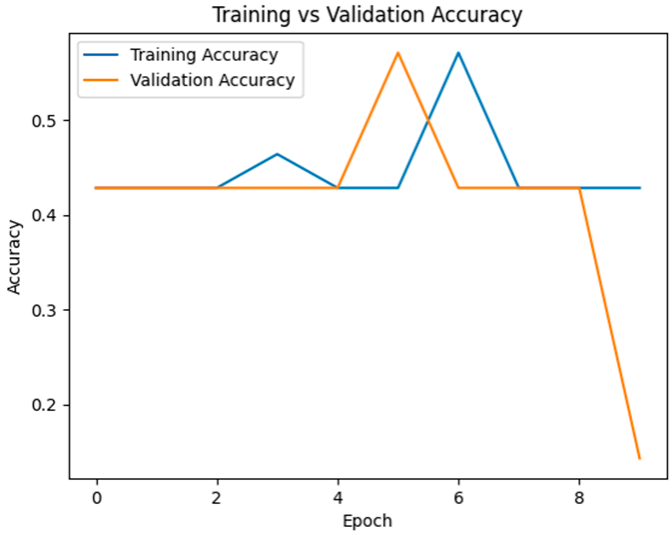


Figure 3. Training and validation accuracy across 10 epochs using the initial limited dataset. Source: author's own work.

3.2. Second Run—Improved Dataset and Epochs

In the second run, the dataset was expanded to include 40 training and 30 testing images, with a more balanced distribution across all three classes. The number of training epochs was increased to 30. As shown in Figure 4, the training accuracy rose significantly (up to ~98%), though validation accuracy fluctuated and plateaued around 50%. This suggests that the model learned well on the training data but may have limited generalisation, potentially due to remaining class imbalance or lack of variability in the test set.

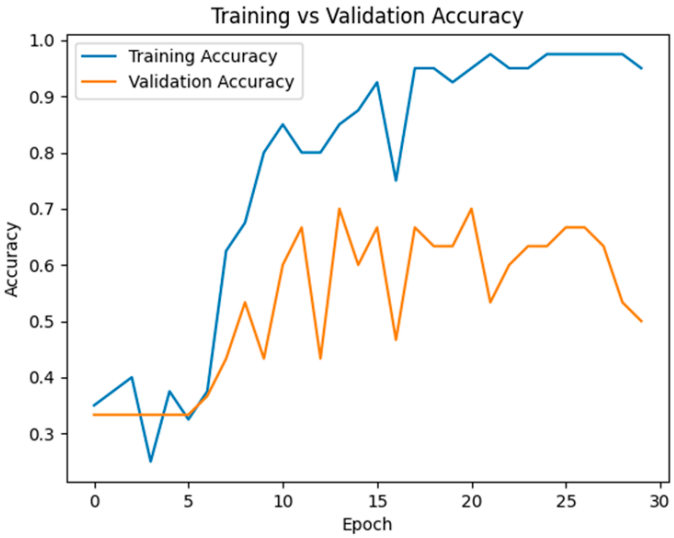


Figure 4. Training and validation accuracy across 30 epochs with the expanded dataset. Source: author's own work.

The model was trained for 30 epochs, after which the validation accuracy plateaued while the training accuracy continued to increase (Figure 4). This indicates that the model begins to overfit beyond this point, as it learns the training data without significant improvements in generalisation. Although increasing the number of epochs to 50 or even 100 could potentially push the training accuracy closer to 100%, it is unlikely to significantly enhance validation accuracy. Instead, such prolonged training may lead to overfitting, where the model performs well on training samples but fails to generalise to unseen data. Future research could explore advanced optimisation strategies such as early stopping, learning rate scheduling, and stronger regularisation techniques to better utilise longer training schedules while mitigating overfitting risks [19].

On the other hand, a key limitation of this study is the relatively small dataset used for training and testing. The positive effect of increasing the dataset size was observed when comparing Run 1 and Run 2: the total number of test images increased from seven to 30, and training images from 34 to 40. This resulted in an improvement in training and validation accuracy from approximately 42% to 64%. This trend suggests that further expanding the dataset would improve the model's learning capability. Larger datasets would provide more representative coverage of microstructural variations, allowing the convolutional neural network to better learn distinguishing features of carbide precipitation. Future work will focus on systematically collecting and annotating a larger number of micrographs to achieve higher accuracy and robustness in practical applications [20].

3.3. Final Evaluation—Classification Report and Confusion Matrix

To assess the model's predictive performance, a classification report and confusion matrix were produced using the independent test dataset after training completion. The classification report, summarised in Table 1, provides precision, recall, and F1-score metrics for each class: as-received, heat-treated without carbides, and heat-treated with carbides. These metrics indicate that the model was moderately successful in distinguishing between the categories, with the highest precision (0.60) observed in identifying samples with no carbides. The overall classification accuracy obtained from the test dataset was 37%, reflecting the model's generalisation performance on unseen data.

Table 1. Classification performance metrics of the machine learning model applied to microstructural image classification. Results include precision, recall, F1-score, and support for each class: as-received, heat-treated (no carbides), and heat-treated (with carbides), along with macro and weighted averages. Source: author's own work.

Class Label	Description	Precision	Recall	F1-Score	Support
0	As-received	0.29	0.50	0.37	10
1	Heat Treatment (no carbides)	0.60	0.30	0.40	10
2	Heat Treatment (with carbides)	0.38	0.30	0.33	10
Overall Accuracy				0.37	0.30
Macro average		0.42	0.37	0.37	30
Weighted average		0.42	0.37	0.37	30

The confusion matrix is detailed in Table 2, which visualises the distribution of true versus predicted labels. The matrix reveals notable misclassifications, particularly between classes 1 and 2, indicating overlapping features in microstructural patterns. Meanwhile,

Figure 5 illustrates the training and validation accuracy over 30 epochs, showing strong learning performance on training data but fluctuating validation accuracy, which may point to model overfitting or limitations in the dataset size and variability.

Table 2. Confusion matrix showing actual versus predicted class outcomes. Each row represents the true class, while each column represents the predicted class, illustrating the distribution of classification results. Source: author's own work.

Confusion Matrix	Predicted: 0	Predicted: 1	Predicted: 2
Actual: 0	5	1	4
Actual: 1	6	3	1
Actual: 2	6	1	3

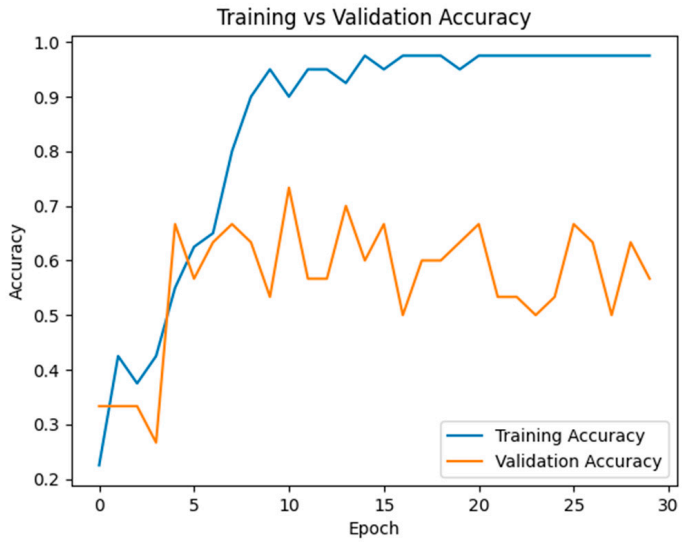


Figure 5. Confusion matrix showing classification outcomes for test samples. Source: author's own work.

These evaluations highlight both the potential and limitations of the current model architecture and dataset. They suggest a need for further refinement, such as expanding the dataset and possibly implementing more advanced CNN layers or regularisation techniques to enhance generalizability.

3.4. Interpretation and Relevance to AM

These results demonstrate the feasibility of using machine learning to automatically classify austenitic stainless-steel microstructures based on carbide presence. Although the model's generalisation is not yet optimal, the learning trend suggests that further improvements can be achieved through data augmentation and more varied training sets.

In the context of AM, the proposed approach offers the potential for real-time microstructure monitoring during layer deposition. By linking the trained model's output to process parameters (such as scan speed, cooling rate, or energy input), manufacturers could adjust AM conditions dynamically to avoid carbide precipitation. This would support the production of high-performance, corrosion-resistant components with tailored microstructures.

This study applied a lightweight image classification model to distinguish between three microstructural states of austenitic stainless steel: as-received, heat-treated without carbide precipitation, and heat-treated with carbide precipitation. The model, trained on a limited dataset, showed clear potential in identifying carbide formation, which is a critical factor influencing corrosion resistance and mechanical reliability in stainless steel components. It should be noted that carbide precipitation is not the only defect influencing

additive manufacturing quality. Other defects, such as lack of fusion and porosity, also play a significant role. However, this study focuses specifically on carbide precipitation due to its critical impact on corrosion behaviour in austenitic stainless steels.

In the context of AM, particularly for metallic systems, controlling microstructural features like carbide precipitation is essential. Excessive carbide formation, especially along grain boundaries, can lead to sensitisation and intergranular corrosion. By incorporating machine learning-based microstructure recognition into the AM pipeline, manufacturers can introduce early-stage, image-based quality control to ensure more consistent output. Other studies [21,22] have demonstrated the effectiveness of combining process parameters, design of experiments, and machine learning models for process optimisation. In contrast, the present study focuses on image-based microstructure classification, providing a complementary approach for evaluating material response, which could be integrated with process-driven models in future work.

It should be noted that the dataset used in this study is relatively small, which may limit statistical robustness and generalisation capability. However, the controlled nature of the microstructures and the clear distinction between classes support the feasibility of the proposed approach. The observed improvement in model performance with increased dataset size further indicates the potential scalability of the method. Future work will focus on expanding the dataset and validating the model under more diverse conditions.

The observed difference between training/validation and test accuracy indicates potential overfitting, primarily due to the limited dataset size. Techniques such as data augmentation, dropout layers, and regularisation (L1/L2) are well-established approaches to mitigate overfitting and improve generalisation. These strategies will be explored in future work to enhance model robustness.

The proposed model demonstrates the potential of automated microstructure evaluation as a post-process quality assessment tool to support process optimisation in additive manufacturing. While not intended for real-time control, this approach provides a foundation for future integration with in situ monitoring and data-driven process optimisation strategies aimed at producing carbide-free austenitic microstructures.

The results of this study also highlight a potential path toward a low-cost, accessible method for microstructural evaluation, especially useful during R&D phases or for small-to-medium enterprises lacking advanced microscopy analysis tools. From a commercial standpoint, integrating this type of model supports the movement toward more automated, reliable, and sustainable manufacturing. This aligns well with Industry 4.0 goals: reducing waste, improving energy efficiency, and enabling real-time process feedback using data-driven tools. Ultimately, the approach offers a scalable pathway for smarter quality assurance in AM, particularly when working with stainless steel components where microstructure critically affects performance.

4. Conclusions

This study demonstrated the feasibility of using a machine learning approach to identify microstructural changes, specifically, carbide precipitation, in austenitic stainless steel (AISI 316) based on image classification. A basic convolutional neural network (CNN) model was trained and tested using optical micrographs categorised into three classes: as-received, heat-treated without carbide formation, and heat-treated with visible carbide precipitation.

The model showed increasing classification performance with improved dataset size and training configuration. Despite working with a relatively small image set, the final results suggest that ML-based microstructure recognition can serve as a rapid and cost-effective tool for early quality assessment in materials processing.

In the context of AM, this approach provides a foundation for intelligent monitoring systems that help mitigate the risk of carbide-related degradation. The proposed approach demonstrates the potential of machine learning for microstructure-based quality assessment and could support future developments in data-driven process optimisation.

While this study successfully demonstrates an AI-driven approach for microstructural classification, it does not yet implement a closed-loop control system within the AM process. The present work should be viewed as an enabling technology for such control. The developed model provides a foundation for future research aiming to integrate microstructure classification with process monitoring systems in additive manufacturing. This would allow dynamic adjustment of heat input, travel speed, and cooling strategies to minimise carbide precipitation during layer deposition. Future research will focus on embedding this classifier into a full closed-loop control framework to actively optimise process parameters and ensure carbide-free microstructures.

Author Contributions: Conceptualization, F.K.; Methodology, F.K.; Software, F.K. and W.Y.; Validation, F.K.; Formal analysis, F.K.; Investigation, W.Y.; Resources, F.K.; Data curation, W.Y.; Writing—original draft, F.K.; Writing—review & editing, F.K. and W.Y. All authors have read and agreed to the published version of the manuscript.

Funding: This research received no external funding.

Data Availability Statement: The original contributions presented in this study are included in the article. Further inquiries can be directed to the corresponding author.

Acknowledgments: The authors thank De Montfort University, United Kingdom, for facilitating and supporting the successful completion of this study.

Conflicts of Interest: The authors declare no conflict of interest.

References

1. Rahmatalla, H.; Khoshnaw, F. Stress corrosion cracking behaviour of welded duplex stainless steel. *Adv. Mater. Res.* **2010**, *89–91*, 709–714. [CrossRef]
2. Khoshnaw, F. *Welding of Metallic Materials: Methods, Metallurgy, and Performance*; Elsevier: Amsterdam, The Netherlands, 2022. [CrossRef]
3. Khoshnaw, F.; Marinescu, C.; Sofronia, A.; Munteanu, C.; Marcu, M.; Barbulescu, L.E.; Ciobota, C.; Cojocaru, E.M.; Tanasescu, S.; Paraschiv, A. Microstructural and thermoanalytical characterization of super duplex stainless steel—UNS S32760-F55. *Mater. Today Commun.* **2021**, *28*, 102644. [CrossRef]
4. Barrionuevo, G.; Rios, S.; Williams, S.W.; Ramos-Grez, J.A. Comparative evaluation of machine learning regressors for the layer geometry prediction in wire arc additive manufacturing. In Proceedings of the IEEE International Conference on Mechatronics, Automation and Robotics (ICMAR), London, UK, 23–25 July 2021; pp. 186–190. [CrossRef]
5. Treutler, K.; Wesling, V. The Current State of Research of Wire Arc Additive Manufacturing (WAAM): A Review. *Appl. Sci.* **2021**, *11*, 8619. [CrossRef]
6. Liu, J.; Xu, Y.; Ge, Y.; Hou, Z.; Chen, S. Wire and arc AM of metal components: A review of recent research developments. *Int. J. Adv. Manuf. Technol.* **2020**, *111*, 149–198. [CrossRef]
7. Xiao, X.; Waddell, C.; Hamilton, C.; Xiao, H. Quality prediction and control in wire arc AM via novel machine learning framework. *Micromachines* **2022**, *13*, 137. [CrossRef] [PubMed]
8. Ladani, L.J. Applications of artificial intelligence and machine learning in metal additive manufacturing. *J. Phys. Mater.* **2021**, *4*, 044001. [CrossRef]
9. Davoodi, F.; Ashrafizadeh, F.; Atapour, M.; Rikhtegaran, R. A novel approach for evaluation of load bearing capacity of duplex coatings on aluminum alloy using PLS and SVR models. *Trans. Nonferrous Met. Soc. China* **2022**, *32*, 1834–1851. [CrossRef]
10. Lee, C.; Seo, G.; Kim, D.B.; Kim, M.B.; Shin, J. Development of defect detection AI model for wire + arc AM using high dynamic range images. *Appl. Sci.* **2021**, *11*, 7541. [CrossRef]
11. Li, Y.; Mu, H.; Polden, J.J.; Li, H.; Wang, L.; Xia, C.; Pan, Z. Towards intelligent monitoring system in wire arc additive manufacturing: A surface anomaly detector on a small dataset. *Int. J. Adv. Manuf. Technol.* **2022**, *120*, 5225–5242. [CrossRef]

12. Tang, S.; Wang, G.; Zhang, H. In situ 3D monitoring and control of geometric signatures in wire and arc additive manufacturing. *Surf. Topogr. Metrol. Prop.* **2019**, *7*, 025013. [CrossRef]
13. Xia, C.; Pan, Z.; Polden, J.; Li, H.; Xu, Y.; Chen, S.; Zhang, Y. A review on wire arc additive manufacturing: Monitoring, control and a framework of automated system. *J. Manuf. Syst.* **2020**, *57*, 31–45. [CrossRef]
14. Oh, W.; Lee, C.; Kim, D. Prediction of deposition bead geometry in wire arc AM using machine learning. *J. Mater. Res. Technol.* **2022**, *20*, 4283–4296. [CrossRef]
15. Kunchala, B.K.R.; Gamini, S.; Anilkumar, T.C. Inclusion of IoT technology in additive manufacturing: Machine learning-based adaptive bead modelling and path planning for sustainable wire arc additive manufacturing and process optimization. *Proc. Inst. Mech. Eng. Part C J. Mech. Eng. Sci.* **2022**, *236*, 12456–12472. [CrossRef]
16. Ding, D.; He, F.; Yuan, L.; Pan, Z.; Wang, L.; Ros, M. The first step towards intelligent wire arc additive manufacturing: An automatic bead modelling system using machine learning through industrial information integration. *J. Ind. Inf. Integr.* **2021**, *23*, 100218. [CrossRef]
17. Abdelal, G.; Chan, C.-W.; McLoone, S. Critical review of recent advances in AI-enhanced SEM and EDS techniques for metallic microstructure characterization. *Appl. Sci.* **2026**, *16*, 975. [CrossRef]
18. Abadi, M.; Agarwal, A.; Barham, P.; Brevdo, E.; Chen, Z.; Citro, C.; Corrado, G.S.; Davis, A.; Dean, J.; Devin, M.; et al. TensorFlow: Large-Scale Machine Learning on Heterogeneous Distributed Systems. *arXiv* **2015**, arXiv:1603.04467. [CrossRef]
19. Ahmed, W.; Ashraf, T.; AlMutairi, D.; Zaman, S.; Ahmed, S.; Ehsan, H. A deep dive into machine learning: The roles of neural networks and random forests in QSPR analysis. *BioNanoScience* **2025**, *15*, 89. [CrossRef]
20. Goodfellow, I.; Bengio, Y.; Courville, A. *Deep Learning*; MIT Press: Cambridge, MA, USA, 2016. [CrossRef]
21. Costa, P.S.; Altamirano, G.; Salinas, A.; Gonzalez, D.S.; Goodwin, F. Optimization of the Continuous Galvanizing Heat Treatment Process in Ultra-High Strength Dual Phase Steels Using Multivariate Model. *Metals* **2019**, *9*, 703. [CrossRef]
22. Rezendiz-Flores, E.O.; Altamirano-Guerrero, G.; Costa, P.S.; Salas-Reyes, A.E.; Salinas-Rodriguez, A.; Goodwin, F. Optimal Design of Hot-Dip Galvanized DP Steels via Artificial Neural Networks and Multi-Objective Genetic Optimization. *Metals* **2021**, *11*, 578. [CrossRef]

Disclaimer/Publisher's Note: The statements, opinions and data contained in all publications are solely those of the individual author(s) and contributor(s) and not of MDPI and/or the editor(s). MDPI and/or the editor(s) disclaim responsibility for any injury to people or property resulting from any ideas, methods, instructions or products referred to in the content.